Journal of South American Earth Sciences 126 (2023) 104331

Contents lists available at ScienceDirect

Journal of South American Earth Sciences

journal homepage: www.elsevier.com/locate/jsames

# Stomatal numbers of *Pseudofrenelopsis capillata* (Cheirolepidiaceae, Coniferales) in the peri-equatorial late Aptian Crato Formation (Santana group, Araripe Basin, Brazil) and their paleoclimatic and paleoenvironmental significance

Isabela Degani-Schmidt [a,*], Margot Guerra-Sommer [a], Ismar de Souza Carvalho [b,c]

[a] Universidade Federal Do Rio Grande Do Sul, IGEO, Programa de Pós-Graduação Em Geociências, Av. Bento Gonçalves 9500, 91509-900, Porto Alegre, RS, Brazil
[b] Universidade Federal Do Rio de Janeiro, CCMN/IGEO, Dept. Geologia, Av. Athos da Silveira Ramos, 274, Bloco J1, Cidade Universitária, 21949-900, Rio de Janeiro, RJ, Brazil
[c] Universidade de Coimbra, Centro de Geociências, Rua Silvio Lima, Coimbra, 3030-790, Portugal

ARTICLE INFO

*Keywords:*
Conifers
Paleoatmospheric $CO_2$
Stomatal proxy
Early Cretaceous

ABSTRACT

This study is the first contribution towards the estimation of paleoatmospheric carbon dioxide concentration ($pCO_2$) from the paleoequatorial late Aptian Crato Formation (Santana Group, Araripe Basin, NE Brazil) based on stomatal numbers. Cuticular and epidermal silicon replicas of *Pseudofrenelopsis capillata* Sucerquia, Bernardes-de-Oliveira & Mohr (Cheirolepidiaceae, Coniferales) were observed under scanning electron microscopy to analyze their stomatal frequency and distribution for paleoatmospheric and paleoenvironmental inferences. Stomatal counting yielded a mean stomatal density (SD) and stomatal index (SI) of 68.8 $mm^{-2}$ and 6.7. Based on the mean SI value of four modern nearest living equivalent (NLE) conifer species, the stomatal ratio (SR) was calculated to be 1.4. The paleoatmospheric $pCO_2$ range was estimated to be between 514.9 ppmv (Recent standardization) and 1029.8 ppmv (Carboniferous standardization). These values were found to be consistent with results from the literature based on other latitudes in the Early Cretaceous and were discussed in the light of the paleoenvironmental context that prevailed around the peri-equatorial Crato paleolake, including the occurrence of stomatal clustering in the leaves of *P. capillata*.

## 1. Introduction

The Phanerozoic eon consists of more than 70% greenhouse climate state, while the Cretaceous period is one of the longest and most studied greenhouse periods in Earth's history (Barral et al., 2017; Kidder and Worsley, 2010). The Cretaceous is characterized by mostly warm polar and tropical temperatures and marked by a gradual warming from the Aptian–Albian to the Cenomanian ages (Chaboureau et al., 2014, and references therein). However, the understanding of the Early Cretaceous climate is still obscured by several paleontological gaps and conflicts between geological and paleontological evidences (Arai and Assine, 2020) and has only a few relative contributions from paleobotanical proxies for reconstructions of paleoatmospheric carbon dioxide pressure ($pCO_2$) for this time interval.

Geochemical and paleontological analyses, including multi-proxy approaches for estimating paleoatmospheric $pCO_2$, showed fluctuations in atmospheric composition and temperature during the Early Cretaceous period, indicating climatic oscillations and a transition into frank greenhouse conditions in the beginning of the Late Cretaceous (Jin et al., 2023). The reconstructions of $pCO_2$ for the late Early Cretaceous period based on stomatal numbers of conifers have so far been obtained for medium to high latitudes only (e.g., Dai and Sun, 2018; Passalia, 2009).

The stomatal frequency in many terrestrial plants is mainly determined by both the carbon dioxide ($CO_2$) uptake and the loss of water vapor. Generally, an inverse correlation exists between stomatal numbers and $pCO_2$, i.e., higher $CO_2$ levels in the atmosphere correspond to lower stomatal numbers and vice versa (Woodward, 1987). Van de Water et al., 1994 demonstrated that this correlation has been very consistent in *Pinus flexilis* for at least the past 30,000 years.

The stomatal index (SI) represents the proportion of stomata in relation to epidermal cells in the leaf surface and is determined to

* Corresponding author.
*E-mail addresses:* degani.schmidt@gmail.com (I. Degani-Schmidt), margot.sommer@ufrgs.br (M. Guerra-Sommer), ismar@geologia.ufrj.br (I.S. Carvalho).

https://doi.org/10.1016/j.jsames.2023.104331
Received 8 February 2023; Received in revised form 27 March 2023; Accepted 2 April 2023
Available online 5 April 2023

minimize the variation in stomatal numbers by the influence of local environmental conditions (Salisbury, 1927). SI can be used to reconstruct past $pCO_2$ by comparing the stomatal numbers of fossil plants to those of their nearest living relatives or equivalents (Aucour et al., 2008; McElwain and Chaloner, 1995). Steinthorsdottir et al. (2022) emphasized that the stomatal proxy is a reliable method to reconstruct $pCO_2$ uniformly and reasonably well; furthermore, it does not systematically underestimate $pCO_2$ under high temperatures like the isotope-based proxy.

Regions with tectonic complexity, such as the Araripe Basin during the late Aptian age, may have become a hotspot of paleobiodiversity shaped by plate tectonics (Bétard et al., 2018; Pellissier et al., 2018), which is of importance for elucidating issues like the angiosperm diversification in the Lower Cretaceous. Therefore, improved knowledge of the paleoclimatic and paleoenvironmental conditions during the late Aptian deposition of the Crato Formation may shed light on the diversification of a rich community of flowering plants, from the magnoliids, and monocots to the core eudicot clade of the angiosperm group (e.g., Mohr et al., 2007).

The present study contributes to the first record of late Aptian $pCO_2$ reconstruction for the paleoequatorial region based on the stomatal numbers of the cheirolepidiacean conifer *Pseudofrenelopsis capillata*

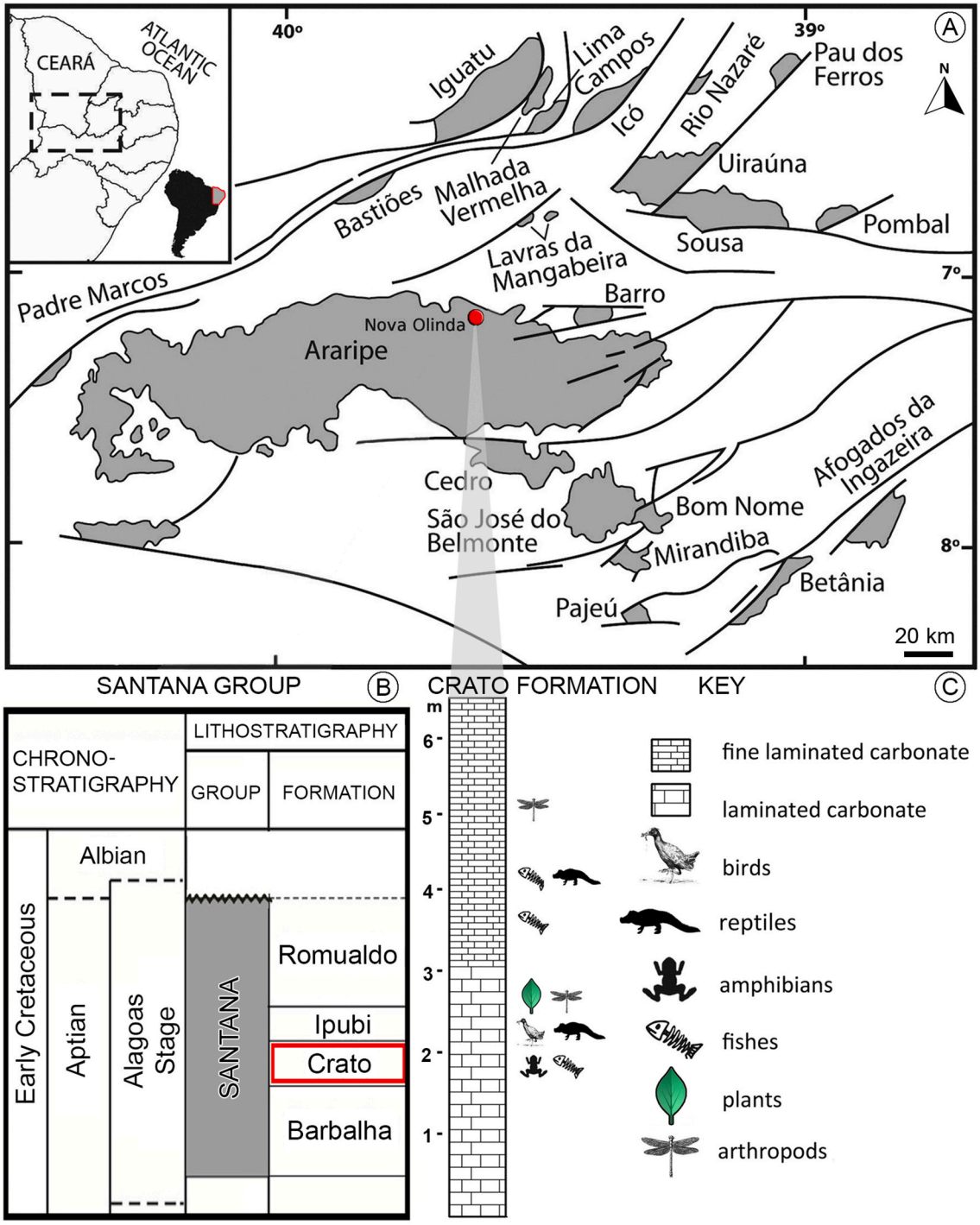


**Fig. 1.** Location map and simplified geological charts. A) Collection site in Nova Olinda County (red circle) and deposits of the Araripe Basin (gray area); B) chronostratigraphic chart (not in scale) of the Santana Group after Arai and Assine (2020); C) lithostratigraphic chart of the outcrops at Nova Olinda County.

Sucerquia, Bernardes-de-Oliveira & Mohr (Crato Formation, Santana Group, Araripe Basin, northeastern Brazil). Furthermore, the study aims to contextualize the results in comparison with other coeval records and to refine the understanding of the paleoenvironmental conditions based on epidermal analysis.

## 2. Geological setting, and paleoclimatic and paleontological context

The Araripe Basin is a hinterland basin related to the South Atlantic opening, and is located in the southern Ceará state, northwestern Pernambuco state, and eastern Piauí state, all in the northeastern Brazil (Fig. 1A). It has a surface area of 12,000 km$^2$, where most outcropping sedimentary successions are Mesozoic siliciclastic and chemical deposits (Assine, 2007; Carvalho, 2000, 2004; Matos, 1992). The lithostratigraphic subdivision of the Araripe Basin has been extensively debated in distinct proposals that were recently reviewed by Fambrini et al. (2020). The chronostratigraphic and lithostratigraphic classifications adopted in this study were those of Arai and Assine (2020), where the late Early Cretaceous Santana Group comprises, from bottom to top, the Barbalha, Crato, Ipubi, and Romualdo formations (Fig. 1B). While still being debated, the Santana Group has been proposed to be of late Aptian age (113–119 Ma) based on the recognition of the palynological subzone P-270-2 (Arai and Assine, 2020; Heimhofer and Hochuli, 2010; Regali and Santos, 1999; Rios-Netto et al., 2012). Recent palynofacies analysis further supports this proposal due to the presence of *Sergipea variverrucata* in all sections (Vallejo et al., 2023). Additionally, the integration of foraminifera (some with Tethyan affinities), ostracode, and other microfossil data from the Romualdo Formation indicated that the local Alagoas Stage (Ostracoda Zone RT-011) can now be constrained to the Aptian (Melo et al., 2020).

The *Pseudofrenopsis* specimens studied came from the limestone succession named Crato Formation (Fig. 1C), which comprises one of the most important Cretaceous fossil Lagerstätten of Gondwana (Martill et al., 2007). It consists of gray, dark brown to black shales and gray to brown laminated limestones and is interpreted as deposited in a continental lake complex during a phase of tectonic quiescence (Neumann et al., 2002).

The cyclic alternation of pale to dark colored carbonate laminae reflects the periods of low to high concentrations of sulfite related to relatively anoxic water conditions (Dias and Carvalho, 2022; Gomes et al., 2021; Varejão et al., 2020). Growth ring analysis of a conifer wood collected from the same carbonate level as the *Pseudofrenopsis* macroremains revealed a pattern linked to a tropical and erratically humid environment, probably due to temporary water stress episodes (Santos et al., 2021).

The occurrence of evaporites in the overlying Ipubi Formation and a consequent general negative precipitation/evaporation rate inferred for the equatorial continental areas during the Aptian age have been considered evidence for the establishment of the Tropical Equatorial Hot arid belt (Chumakov et al., 1995; Sewall et al., 2007). However, alternation of humid and dry cycles, probably associated with seasonal precipitation, have been proposed for the heterolytic succession in the Santana Group based on sedimentological, paleontological, and organic matter evidence (Neumann et al., 2003; Ribeiro et al., 2021; Scherer et al., 2015). Additionally, based on a fully coupled ocean-atmosphere general circulation model (FOAM), Chaboureau et al. (2014) estimated a positive precipitation/evaporation rate for the Aptian Tropical Equatorial belt in northern Brazil, with heavy rainfalls typical of monsoon systems. Both the Tethys and the Pacific oceans would have supplied moisture to the region via trade and south-westerly winds during most part of the year.

Evidence from macrofloral remains also contradicts the presumed prevalence of strict arid conditions (Bernardes-de-Oliveira et al., 2014). Comparative analysis of growth patterns in conifer woods from the Crato and Romualdo formations showed climatic oscillations from an erratically humid environment in the lower Crato Formation to a relatively humid environment in the upper Crato Formation, until the establishment of a distinct post-evaporitic monsoon-like climate during the deposition of the overlying Romualdo Formation (Guerra-Sommer et al., 2021). This result agreed with the FOAM model by Chaboureau et al. (2014) and attests to the successful refinement of paleoclimatic events through paleobotanical data.

Souza-Lima and Silva (2018) reported through their palynology review that the plant diversity in the Crato Formation included 14 angiosperm and 12 gymnosperm families (half of which were conifers), besides 18 hygrophyte-hydrophyte families of ferns and bryophytes. Carvalho, M. et al. (2022) detected oscillations in these abundances along the formation, and Hofmann et al. (2022) reported 21 different gnetalean pollen types from the lowermost level of the Crato Formation. In a macrofossil review conducted by Ribeiro et al. (2021) for the paleoenvironmental reconstruction of the Crato Konservat-Lagerstätte as a shallow lacustrine wetland, the taxonomic composition of the paleobotanical macroremains was interpreted to be 44% terrestrial herbaceous (xeric, e.g., Gnetales), 14% arboreal (dry habitat, some conifers), 14% helophytes/amphiphytes (transitional environments, e.g., Equisetales), 11% hydrophytes (e.g., Nymphaeales), 11% terrestrial herbaceous (mesophytic, e.g., ferns), and 6% arboreal (riparian habitat, e.g. *Pseudofrenelopsis*).

The discovery of freshwater to brackish genera of Ostracoda trapped in amber and in the surrounding limestone was associated with the predominance of *Classopollis* pollen, which demonstrates the occurrence of the Cheirolepidiaceae family in the Crato Lake margins (Piovesan et al., 2022). These findings additionally corroborated previous paleoenvironmental reconstructions (Neumann et al., 2003; Ribeiro et al., 2021) and led to inferences of significant, although intermittent, humidity inputs favorable to the growth of arboreal plants (Santos et al., 2020).

## 3. Material and methods

The five analyzed specimens were collected from the Três Irmãos and Pedra Branca limestone quarries in the Nova Olinda County, Ceará state (northeast Brazil, Fig. 1). Cuticular and epidermal silicon replicas of *Pseudofrenelopsis capillata* leaves were obtained from compressed specimens (Fig. 2) composed of goethite (Prado et al., 2020). The casts of the plant surfaces were produced with dental silicone (Moisan, 2012), which were then glued on glass slides, gold coated, and observed under two scanning electron microscopes (SEM), Inspect F50 FEI located at the Centro de Microscopia e Microanálises at Pontifícia Universidade Católica do Rio Grande do Sul (IDEIA/PUCRS) and JEOL JSM-6610LV located at the Laboratório de Geologia Isotópica (CPGq/IGEO/UFRGS) in Porto Alegre, RS, Brazil.

Stomatal and epidermal cell counting was performed using a 0.09 mm$^2$ (300 × 300 μm) grid superimposed on the SEM images, avoiding the leaf extremities where the stomatal frequencies were too variable. A total of 163 grids were counted from 38 leaves.

Stomatal density (SD) was determined by manually marking the number of stomata on the computer screen and dividing them by the area of the observed field to obtain the number per square millimeter (Salisbury, 1927). SI was calculated as $SI = 100S/(E + S)$, where S and E represent the numbers of stomata and epidermal cells per unit area, respectively (Salisbury, 1927; Kerp, 1990). This formula expresses the stomatal numbers independent of the epidermal cell size to compensate for the effects of leaf expansion (Poole and Kürchner, 1999).

Stomatal ratio (SR) allows semi-quantitative estimation of paleoatmospheric $CO_2$ based on the inverse correlation between SI and atmospheric $CO_2$ levels. SR can be calculated by dividing the SI of the nearest living equivalent (NLE) by that of the fossil (McElwain and Chaloner, 1995, 1996; McElwain, 1998). The NLE adopted in this study was proposed in Dai and Sun (2018) for *Pseudofrenelopsis papillosa* (Chow et Tsao) Cao ex Zhou based on the data of Haworth et al. (2005,


**Fig. 2.** Some of the studied samples of *Pseudofrenelopsis capillata*. A) UFRJ-DG 2113-Pb; B) UFRJ-DG 2418-Pb; C) UFRJ-DG 2430-Pb. Scale bars = 3 cm.

2010), who calculated a mean SI of 9.2 ± 1.2 for four extant conifer species from different latitudes (*Tetraclinis articulata* (Vahl) Masters, *Callitris rhomboidea* R.Br. Ex Rich. & A.Rich., *Callitris columellaris* F. Muell., and *Athrotaxis cupressoides* D.Don).

According to Chaloner and McElwain (1997) and McElwain (1998), the resulting SR obtained by the Recent and Carboniferous standardizations yields the minimum and maximum paleoatmospheric $CO_2$ values. The Recent standardization establishes a $CO_2$ ratio of 1:1 to the pre-industrial atmospheric level (PIL = 300 ppm; 1SR = $1RCO_2$), while the Carboniferous standardization establishes a 1:2 ratio of PIL (1SR = $2RCO_2$). The calculated semi-quantitative range can then be plotted on the global $CO_2$ curve which is drawn from isotopic and geochemical data and other stomatal estimations available in the literature (McElwain, 1998; McElwain and Chaloner, 1995, 1996). For comparison with preterit levels, the actual $CO_2$ level considered in this study was 373.6 ppm, under which the NLEs lived (average value as determined by Dai and Sun, 2018).

Zeiss AxioVision 4.8 software was used to record measurements, Adobe Photoshop CS6 and Microsoft Excel spreadsheets were used to count and generate the data, respectively. The figures were created using Adobe Photoshop CS6. Transformations made to the images included adjustments in cropping, rotation, and brightness and contrast.

The considered specimens and silicon replicas were housed in the paleontological collection of the Departamento de Geologia, Instituto de Geociências, Universidade Federal do Rio de Janeiro under the acronyms UFRJ-DG 1581-Pb, UFRJ-DG 2113-Pb, UFRJ-DG 2235-Pb, UFRJ-DG 2418-Pb, and UFRJ-DG 2430-Pb.

## 4. Results

The studied specimens consisted of articulated shoots 0.56–1.17 cm wide. Leaves squamiform, one per node, enclosing the cylindrical shoots completely, with oblique, free apical margin ending in dense unicellular 221 μm (110–287 μm) long hairs and no visible suture. Rarely preserved cuticle with papillate epidermal and subsidiary cells (Fig. 3A and B). Abaxial epidermis displayed stomata in longitudinal, mostly well-defined and generally uniseriate files, adjacent or separated by 1–3 ordinary epidermal cells, 8 (6–10) files $mm^{-2}$ (Fig. 3). Circular to ellipsoid stomatal apparati (Fig. 3B) 79.8 μm (64.8–91.6 μm) long and 73.5 μm (67.5–81.9 μm) wide, composed of 5–6 trapezoidal subsidiary cells measuring 36.2 × 22.1 μm (27–44 × 14–29 μm). These features agree with the diagnosis of *P. capillata* made by Sucerquia et al. (2015). Guard cells were not observed, but according to Sucerquia et al. (2015) they are elongated with inner straight edges.

The counted mean SD was 68.8 ± 33 $mm^{-2}$ (53.3–100 $mm^{-2}$) and SI was 6.7 ± 0.9 (5.7–7). The calculated SR was 1.4, yielding an estimated mean $pCO_2$ of 514.9 ± 79 and 1029.8 ± 158 ppmv following the Recent and Carboniferous standardizations, respectively (Table 1).

## 5. Discussion

### 5.1. Stomatal numbers, $pCO_2$ estimates, and temperature

The stomatal numbers of the extant conifers that yielded the mean SI of the NLE are presented in Table 2, and those of the fossil conifer species from the late Early Cretaceous period comparable with *P. capillata*. The fossil conifers were the cheirolepidiacean *Pseudofrenelopsis* spp., *Frenelopsis* spp. and *Tomaxellia* spp., mixed araucariacean/cheirolepidiacean genera *Brachyphyllum* spp., and araucariacean *Nothopehuen brevis* Del Fueyo, considering their similarities both at the morphological level and stomatal numbers (Dai and Sun, 2018; Du et al., 2016; Passalia, 2009). The various SIs of the NLEs utilized in the comparison studies can be found in the compilation made by Du et al. (2016).

The comparison of the stomatal numbers (Table 2) showed that the SD of *P. capillata* calculated in this study (68.8 $mm^{-2}$) is 30.4% lower than the average of the compared results (89.7 $mm^{-2}$). Most results (7 out of 11 calculated average SDs) showed higher SDs (147.6; 86.3; 56.5; 130; 147.5; 64.8; 77.7; 92.6; 47; 65; and 71.2 $mm^{-2}$). The SI of *P. capillata* (6.7) is 8% higher than the average (6.2) of all compared results (9.2; 5.5; 4.6; 7.9; 6.9; 5.5; 6.1; 6.1; 6; 6.1; and 4.6), reflecting a relatively lower estimated $pCO_2$. Only two SI results were higher among the compared fossils, those of the Albian species *Frenelopsis turolensis* (7.9) and *F. alata* (6.9) from Spain and France (Aucour et al., 2008).

The mean of six paleo-$pCO_2$ estimates, including that of the present study (NLE aside), showed a standard deviation of ±110 ppmv; when compared to the paleoestimate average, the present result is 9.1% lower. Considering that the compared studies dealt with material emerging from different latitudes and ages within the late Early Cretaceous period, the results were strikingly congruent among the analyzed conifers. All paleo-$pCO_2$ results from the comparison studies are plotted in Fig. 4.

From the results obtained for the Early and mid-Cretaceous periods by Haworth et al. (2005) based on the stomatal analysis of *Pseudofrenelopsis parceramosa* (Fontaine) Watson (the Wealden and Lower Greensand groups, SW England, and the Potomac Group of Virginia, USA), those of Aptian age were selected for calculating average SD, SI, and $pCO_2$ values for comparison in Table 2 (complete results are shown in Fig. 4). The data suggest a small decrease in $pCO_2$ in the early Barremian and a slight rise after the Aptian–Albian boundary (Fig. 4). The mean $pCO_2$ result for the Aptian was approximately 940 ppmv, which is 22% higher than that obtained in present study from the paleoequatorial region, with a higher SD and a lower SI (average SD = 86.3 $mm^{-2}$ and average SI = 5.5).

Aucour et al. (2008) analyzed the stomatal numbers and $\delta^{13}C$ in three different frenelopsid species and found that the differences were

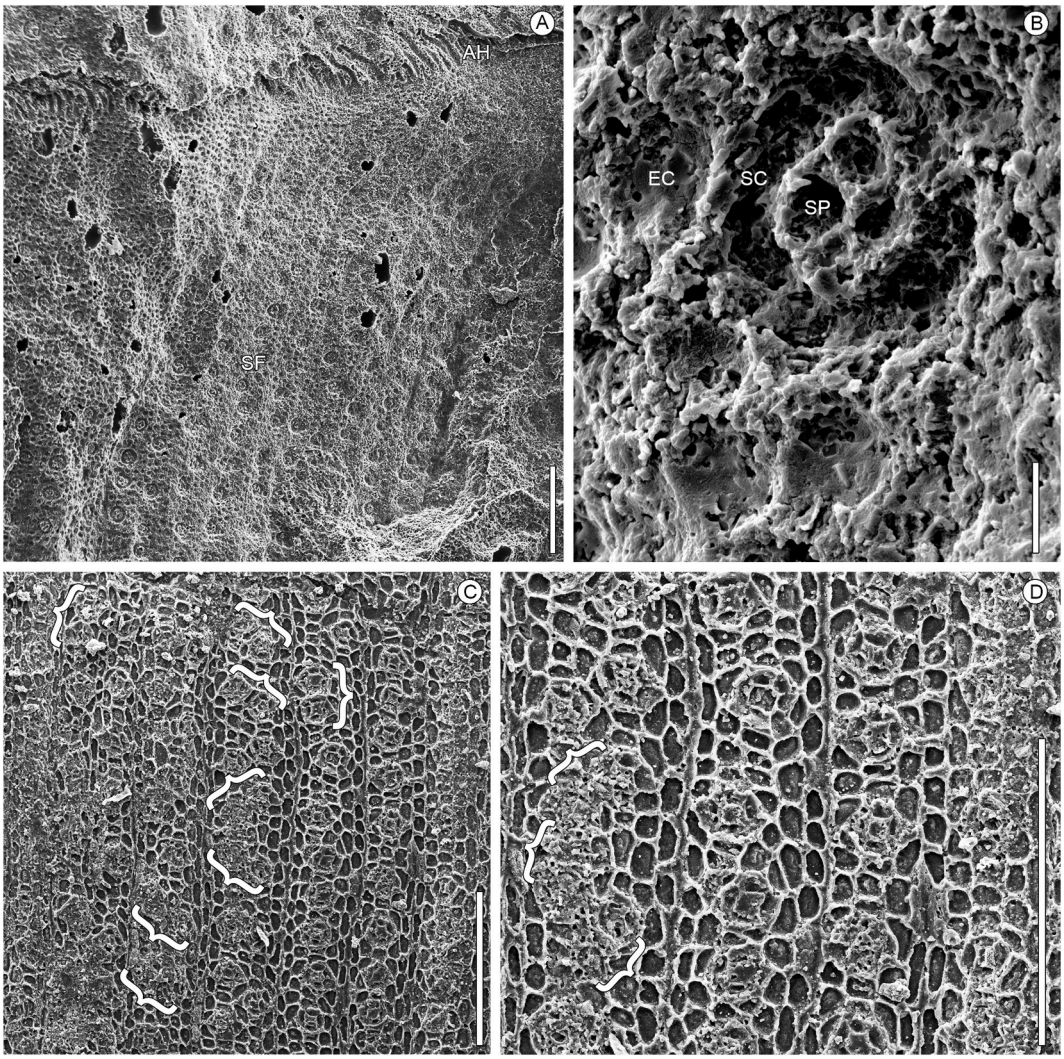


**Fig. 3.** *Pseudofrenelopsis capillata*: silicon casts of leaf cuticle and epidermis under scanning electron microscopy. A) General view of the cast of the outer cuticular surface showing the oblique apical margin with hairs (AH) and stomatal files (SF) (UFRJ-DG 2113-Pb-22); B) detail of the cuticular cast showing papillate epidermal and subsidiary cells (EC = epidermal cell; SC = subsidiary cell; and SP = papilla of subsidiary cell) (UFRJ-DG 2113-Pb-22); C) cast of the outer epidermal surface showing stomatal files, where clustered stomata are indicated by {} (UFRJ-DG 2418-Pb-17); D) details of (C). Scale bars (A, C, D) = 400 μm; (B) = 20 μm.

**Table 1**
Counting results of epidermal cell density, stomatal density, and stomatal index (SI) of *Pseudofrenelopsis capillata* from the Crato Formation and their corresponding calculated stomatal ratio and paleo-$pCO_2$ following the Carboniferous and Recent standardizations (std). Field size = 0.09 $mm^2$; Recent $pCO_2$ = 373.6 ppmv; nearest living equivalent mean SI = 9.2 ± 1.2.

| *Pseudofrenelopsis capillata* – Crato Fm. | [a]Epid. Cell density ($mm^{-2}$) ± σ | [b]Stomatal density ($mm^{-2}$) ± σ | [a]Stomatal index ± σ | Stomatal ratio | $pCO_2$ Recent std (ppmv) ± σ | $pCO_2$ Carbonif. std (ppmv) ± σ |
|---|---|---|---|---|---|---|
| **Min.** | 736.1 | 53.3 | 5.7 | 1.3 | 491 | 982 |
| **Max.** | 1206.7 | 100 | 7 | 1.6 | 603 | 1206 |
| **Mean** | 923.9 ± 174.6 | 68.8 ± 33 | 6.7 ± 0.9 | 1.4 | 514.9 ± 79 | 1029.8 ± 158 |

σ = standard deviation.
[a] n = 2 specimens, 5 leaves, 27 grids.
[b] n = 5 specimens, 38 leaves, 163 grids.

mostly due to changes in environmental salinity rather than oscillations in $pCO_2$. The lower SD (56.5 $mm^{-2}$) of *Frenelopsis ugnaensis* from freshwater deposits in upper Barremian strata of the La Huérgina Formation, besides a more negative $\delta^{13}C$, indicated that this species would have thrived under warmer and drier conditions and lower salinity than the other ones analyzed by the authors. Under lower salinity, the osmotic pressure of the soil's water allowed expansion of the epidermal cells of *F. ugnaensis*, which reduced the stomatal count. The average of their $pCO_2$ results was approximately 698 ppmv, which is only slightly lower than ours, with matching episodes of increased evaporation and likely low salinity.

The study by Passalia (2009) recognized significant $pCO_2$ variations with an approximate mean of 888 ppmv during the middle-late Aptian (approximately 118–114 Ma, according to the radiometric ages later obtained by Césari et al. (2011) and Pérez-Loinaze et al. (2013) for the Anfiteatro de Ticó and Punta del Barco formations, respectively), and

**Table 2**
Comparison of mean stomatal numbers of the nearest living equivalent, the Early Cretaceous fossil species compatible with *Pseudofrenelopsis capillata* (see text for selection criteria), and the corresponding calculated mean $pCO_2$ (modified from Du et al., 2016). NB: the stomatal index of the nearest living equivalents varies among studies.

| Conifer species | Mean SD ($mm^{-2}$) | Mean SI | Mean $pCO_2$ (ppmv) | Age/Locality | Author |
|---|---|---|---|---|---|
| NLE spp. *Tetraclinis articulata*; *Callitris rhomboidea*; *Callitris columellaris*; *Athrotaxis cupressoides* | 147.6 | 9.2 | 373.6 | extant from Morocco, Oceania, and the UK | Dai and Sun (2018); Haworth et al. (2010) |
| *Pseudofrenelopsis parceramosa* | 86.3 | 5.5 | ~940 | middle Aptian Wealden, Lower Greensand (SW England), and Potomac (E USA) groups | Haworth et al. (2005) |
| *Frenelopsis ugnaensis*; | 56.5 | 4.6 | ~698 | late Barremian and Albian from La Huérgina (E Spain) and Escucha (E Spain and W France) formations | Aucour et al. (2008) |
| *F. turolensis*; | 130 | 7.9 | | | |
| *F. alata* | 147.5 | 6.9 | | | |
| Average | 111.3 | 6.5 | | | |
| *Brachyphyllum* spp.; | 64.8 | 5.5 | ~888 | middle–late Aptian from Baqueró Group (S Argentina) | Passalia (2009) |
| *Tomaxellia* spp.; | 77.7 | 6.1 | | | |
| *Nothopehuen brevis* | 92.6 | 6.1 | | | |
| Average | 78.4 | 5.9 | | | |
| *Brachyphyllum* spp.; | 47 | 6 | ~777 | late Aptian–early Albian Zhonggou Formation (NW China) | Du et al. (2016) |
| *Pseudofrenelopsis* spp. | 65 | 6.1 | | | |
| Average | 56 | 6 | | | |
| *Pseudofrenelopsis papillosa* | 71.2 | 4.6 | ~981.5 | late Aptian Junkou Formation (SE China) | Dai and Sun (2018) |
| ***Pseudofrenelopsis capillata*** | **68.8** | **6.7** | **~772.4** | **late Aptian Crato Formation (NE Brazil)** | **present study** |

the highest mean among all compared results in the late Albian–Cenomanian of approximately 986 ppmv (Fig. 4). In Table 2, results from Passalia (2009) from the middle–late Aptian conifers only were considered, and in Fig. 4, his results were plotted according to the new radiometric ages. Their $pCO_2$ result for the Aptian is 15% higher than ours, with a higher mean SD (78.4 $mm^{-2}$) and a lower SI (6). These results were probably linked to a warming process extending towards high latitudes and are consistent with the high floristic diversity recorded in Patagonia during the middle Cretaceous. The fossils analyzed by Passalia (2009) were derived from freshwater deposits with no indication of water stress conditions and were thus consistent with those from the late Barremian (La Huérgina Formation) of Aucour et al. (2008) in the correlation of lower stomatal numbers with lower salinity.

Du et al. (2016) analyzed different cheirolepidiacean species (*Brachyphyllum* spp. and *Pseudofrenelopsis* spp.) occurring across successive fluvial strata along the Aptian–Albian boundary and indicated tropical to subtropical conditions at a high latitude, just like the material studied by Passalia (2009). They found that stomata numbers were more sensitive to $pCO_2$ variations, whereas $\delta^{13}C$ values correlated better with environmental conditions. Du et al. (2016) documented $pCO_2$ fluctuations along the studied interval with a decreasing trend towards the boundary (Fig. 4), closely matching the counted and calculated results presented herein, indicating a reliable identification of global $pCO_2$ by the analyzed conifers, irrespectively of latitude.

The results of Aptian age (112–116 Ma, Junkou Formation, SE China) from the study by Dai and Sun (2018) on *Pseudofrenelopsis papillosa* were considered for comparison in Table 2, which ranged between 753 and 1210 ppmv (second highest mean with approximately 981.5 ppmv) and are 27% higher than ours (complete $pCO_2$ results presented in Fig. 4), with a higher mean SD (71.2 $mm^{-2}$) and a lower mean SI (4.6). Based on the assumed coupling between $pCO_2$ and temperature, Dai and Sun (2018) calculated an increase of approximately 3.6–5.5 °C in the global mean land surface temperature from the late Aptian age, which is in disagreement with the curve of sea surface temperature based on nannofossils of the western Tethys (Fig. 4A), which prevailed at supra-regional scale according to Bottini and Erba (2018), and with the multi-proxy based global average temperature curve of Scotese et al. (2021). However, the raise in temperature may have likely reflected one of the many $pCO_2$ and temperature fluctuations reported for the studied time interval.

A close correlation was perceived between the high-resolution curve of sea surface temperature by Bottini and Erba (2018; Fig. 4A) and the low-resolution GEOCARBSULF curve by Berner (2006, 2008; Fig. 4B), showing that despite several fluctuations, a positive correlation between temperatures and $pCO_2$ may have taken place during most of the Aptian age. The lowest temperature of 29 °C, as estimated by Bottini and Erba (2018) for the western Tethys surface in the late Aptian age (Fig. 4A), corresponds to the speculative Aptian–Albian Cold Snap (AACS) associated with the Carswell impact (115 Ma), for which Scotese et al. (2021) proposed 19 °C as the global average temperature.

Regarding the AACS, the $pCO_2$ estimated for the latest Aptian age by Haworth et al. (2005) reflected a slightly decreasing trend; Du et al. (2016) and Passalia (2009) showed a marked $pCO_2$ decrease and the present result was the lowest mean $pCO_2$ estimated for the late Aptian age, which is similar to the results by Du et al. (2016) and Passalia (2009). Among the geochemical models compared in this study, the results by Tajika (1999) showed a marked decline in the $pCO_2$ of the late Aptian, which also coincided with the temperature curve and with the Carboniferous standardization of most stomatal proxies. Therefore, these results fit in the cooling theory, as can be seen in Fig. 4. It is important to contextualize that many studies indicated that the mid-Cretaceous greenhouse conditions were not continuous and had several cooling interludes (Bottini and Erba, 2018; and references therein).

Nevertheless, a decoupling between $pCO_2$ and temperature has been recognized during the Early Cretaceous by Barral et al. (2017). Based on carbon isotope compositions of the fossil conifer *Frenelopsis*, with results ranging ca. 150–650 ppmv in the Barremian–Santonian, Barral et al. (2017) observed drastic Myr-scale $pCO_2$ drawdowns during time intervals inferred as the warmest for the Cretaceous: - ca. 310 ppmv during the late Barremian–early Aptian interval (ca. 7.5 Myr); and - ca. 225 ppmv during the late Albian–early Cenomanian interval (ca. 5 Myr). Even inverse trends in $pCO_2$ and temperature were observed by these and other authors during significant time intervals throughout the Early and mid-Cretaceous and the status of $pCO_2$ as the main long-term driver of global warming during the Cretaceous has been questioned (Barral et al., 2017; Davis, 2017 and references therein; Erba et al., 2015; Steinthorsdottir et al., 2022). This partial mismatch observed in Fig. 4 between the temperature curve by Bottini and Erba (2018) and biogeochemical carbon cycle curve modeled by Tajika (1999) confirms the timing of $pCO_2$ and temperature decoupling recognized by Barral et al. (2017).

Mora et al. (2021) tested the photosynthetic homeostasis of Aptian

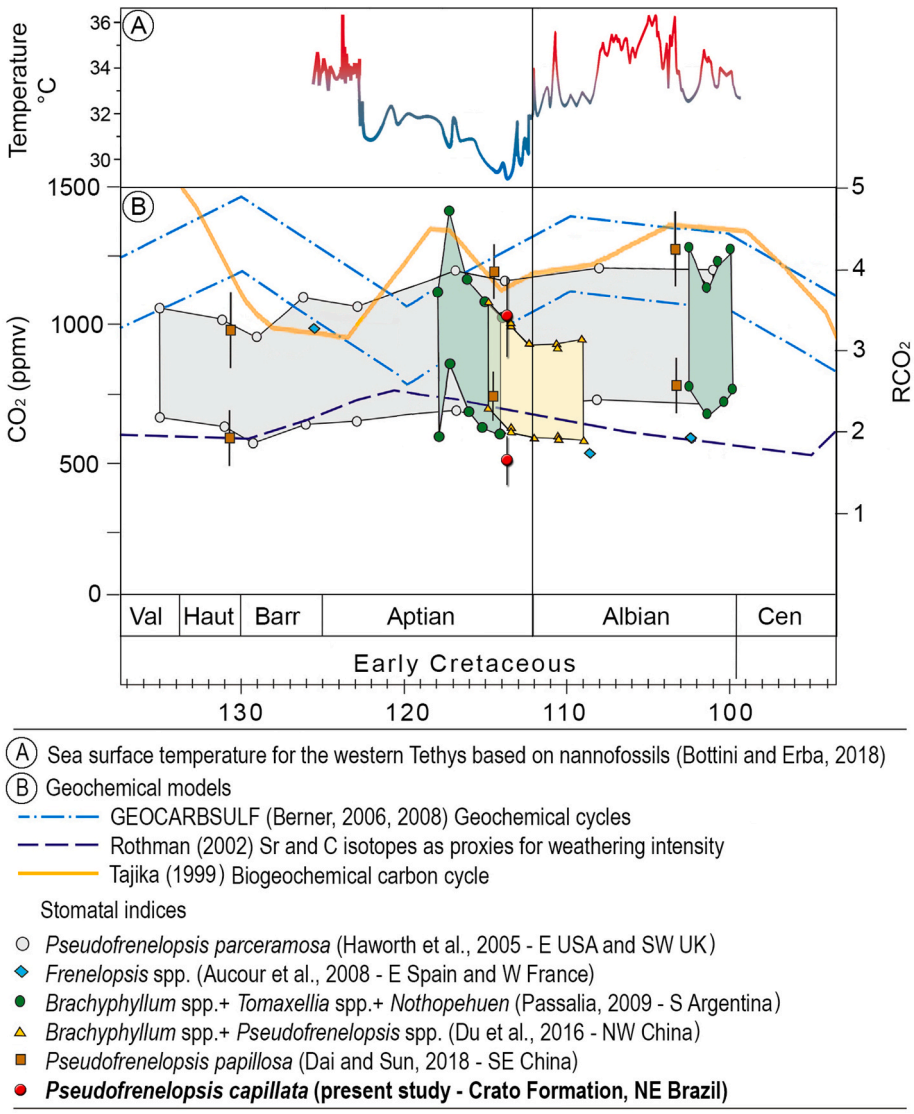


**Fig. 4.** Comparison of Early Cretaceous estimates of temperatures and $pCO_2$. A) Sea surface temperature for the western Tethys based on nannofossils (Bottini and Erba, 2018); B) $pCO_2$ estimates based on geochemical models (Berner, 2006, 2008; Rothman, 2002; Tajika, 1999) and stomatal indices of conifers (Table 2) (modified from Dai and Sun, 2018 and Jin et al., 2023).

conifers by using $\delta^{13}C$ of n-alkanes, cuticles, and bulk organic matter (Potomac Group, Maryland, NE United States) and found similarity with modern relatives, concluding that the processes responsible for regulating $CO_2$ and water vapor exchange during photosynthesis have remained unaltered in gymnosperms at least for the past 128 Ma. Comparisons among the available paleobotanical proxy methodologies for reconstruction of $pCO_2$ suggest that the best resolution is achieved by the stomatal ratio (NLE) approach, while transfer functions or mechanistic approaches that incorporate other variables such as the carbon isotopic composition of leaves (e.g., the Franks model, Franks et al., 2014) disturb the results, leading to an underestimation of $pCO_2$ levels (Barclay and Wing, 2016; Steinthorsdottir and Vajda, 2015; Steinthorsdottir et al., 2021).

The stomatal numbers obtained in the present study from *P. capillata* yielded a 9.1% lower $pCO_2$ than the average results from other conifers during the Aptian–Albian interval. If coupling between $pCO_2$ and temperature was in place at that point in time, our results would correlate well with the low temperatures estimated by Bottini and Erba (2018) and Scotese et al. (2021).

### 5.2. Paleoenvironmental conditions and stomatal distribution

The frequent occurrence of evaporites along the evolving South Atlantic rift system, absence of coal layers, and widespread occurrence of drought-resistant xerophytic vegetation (Mohr et al., 2007; Ziegler et al., 2003) indicate conspicuous semi-arid to arid climatic conditions for the Aptian deposition interval in the Araripe Basin, included in the Tropical Equatorial Hot arid belt by Chumakov et al. (1995).

Based on some sedimentological and paleobotanical (cuticular analysis) evidence, the cheirolepidiaceous conifers have mostly been interpreted as xeromorphic plants adapted to halophytic habitats (Alvin, 1982; Deng et al., 2005; Yang and Deng, 2007). They thrived in open and sunny lowland areas, near water bodies (lake or coastal marine), and on well-drained to dry soils (Vakhrameev, 1981). Their preferred habitat would thus be coastal, riparian, or marshy sandy regions of saline or brackish, low-lying water bodies under subtropical or tropical climate (Piovesan et al., 2022; and references therein). However, this family was cosmopolitan and grew in different environmental scenarios, from arid to humid climates in either continental or seashore environments at low and high latitudes (Llorens et al., 2020).

Cuticular analysis performed by Sucerquia et al. (2015) on

*P. capillata* from the Crato Formation revealed heavily papillated cells, including stomatal pits covered by the solid, round papillae of the subsidiary cells. These adaptations to a semi-arid to arid climate support a scenario of significant evaporation.

Xeromorphic adaptations were also reported for other conifers derived from the Crato Formation. *Brachyphyllum* spp., for instance, had reduced leaves, thick tracheid walls, and thick cuticle (Batista et al., 2021). Mohr et al. (2012) described *Duartenia araripensis* Mohr, Schultka, Süss & Bernardes-de-Oliveira with coriaceous *Brachyphyllum*-type leaves bearing trichomes and a twisting growth pattern in the last-order branches resembling shoot thorns, which are features consistent with extant drought-resistant plants. *Tomaxellia biforme* Archangelsky, another cheirolepidiaceous conifer from the Crato Formation, had rather thick leaves (Kunzmann et al., 2006). In the Crato Formation, such adaptations have been considered to be an environmental response to salinity and aridity conditions (Batista et al., 2021; Ribeiro et al., 2021).

Analysis of wood growth patterns from the laminated lacustrine limestone of the Crato Formation revealed the absence of true growth rings and the common presence of wood growth interruptions, likely linked with a tropical, equable but erratically humid environment (Guerra-Sommer et al., 2021). Moreover, the occurrence of ostracods preserved in amber and the associated dominance of the *Classopollis* pollen suggested that the cheirolepidiaceans of the Crato Formation inhabited a periodically flooded marginal zone of the paleolake (Piovesan et al., 2022).

Besides xeromorphic features of the cheirolepidiaceaeans, this study observed the frequent occurrence of non-contiguous stomatal clustering (guard cells of different stomata do not touch; Fig. 3C and D). A correlation between stomatal clustering in terrestrial plants and environmental signals has been suggested based on increased occurrences of stomatal clustering along drought and salt gradients (Gan et al., 2010). In eudicots, stomatal clusters may assist in water conservation because plant populations were growing under limited water supply and had larger clusters than those growing on well-watered soil substrates (Hoover, 1986). Stomatal clusters were observed in more than 60 extant species of gymnosperms, eudicots, and monocots (Metcalfe and Chalk, 1979).

A stomata-free region is usually observed around each stoma (at least one intervening epidermal cell is always placed between two neighboring pairs of guard cells), which minimizes the overlaps of stomatal gaseous diffusion shells (stomatal chambers) and ensures the optimal balance between water loss and carbon assimilation (Korn, 1993; Larkin et al., 1997). While greater stomatal closure existed in species with the highest SD (El-Sharkawy et al., 1985), non-contiguous stomatal clusters may reduce leaf transpiration and keep water loss at a lower level by the overlapping of the gaseous diffusion shells (Gan et al., 2010).

Although there was salinity variation in the Crato Lake (Ribeiro et al., 2021), the low SD found in *P. capillata* suggests freshwater environment, as per Aucour et al. (2008). Among the environmental factors affecting the stomatal distribution (Barclay et al., 2007), exposure to constant solar radiation and high temperatures all year around in a peri-equatorial latitude was the most profound in the case of *P. capillata*. Temperature-induced increases in plant transpiration were expected because a decrease in leaf temperature causes stomata to open and increase evaporation rates (Jones, 2004). Therefore, both the lower SD and the stomatal clustering are advantageous.

## 6. Conclusions

The first estimation of paleoatmospheric $CO_2$ from the late Aptian peri-equatorial region based on the stomatal numbers of the conifer *Pseudofrenelopsis capillata* (Cheirolepidiaceae) yielded a range of 514.9 $\pm$ 79–1029.8 $\pm$ 158 ppmv (mean $pCO_2$ values from the Recent and the Carboniferous standardizations, respectively). This estimate is consistent with previous findings of stomatal proxies at various latitudes during the Early Cretaceous period.

A high degree of uniformity in the stomatal parameters of cheirolepidiacean conifers was found irrespective of latitude, especially those living in freshwater environments with a trend towards lower SD, as was the case with *P. capillata*. Additionally, the described stomatal clustering could relate to the negative precipitation/evaporation rates that likely prevailed, episodically, during the deposition of the Crato Formation. Therefore, variation in stomatal distribution and density in Early Cretaceous conifers was probably correlated with oscillating salinity and dry/wet environmental conditions.

The SI was found to be inversely correlated with paleoatmospheric $CO_2$ levels with a high degree of confidence. The results represented a screenshot of lower $pCO_2$ values relative to the compared estimates. If coupling between $pCO_2$ and temperature was in place during the late Aptian, our results fit well with the relatively low temperature estimates for that poin in time.

Filling the existing gaps in the Early Cretaceous paleoclimatic and paleoenvironmental reconstructions is a continuous work that would help clarify the conditions in a hothouse world that supported conifer forests at a peri-equatorial latitude and subsequent high diversification in flowering plants.

## Funding

This study was financially supported by Conselho Nacional de Desenvolvimento Científico e Tecnológico (CNPq), Brazil (I.D.S. 150517/2022-0; M.G.S. 304856/2019-3; I.S.C. 303596/2016-3) and Fundação Carlos Chagas Filho de Amparo à Pesquisa do Estado do Rio de Janeiro (FAPERJ), Brazil (I.S.C. E−26/200.828/2021).

## CRediT authorship contribution statement

**Isabela Degani-Schmidt:** Visualization, Validation, Methodology, Investigation, Formal analysis, Data curation, Writing - original draft, Writing - review & editing. **Margot Guerra-Sommer:** Supervision, Conceptualization, Writing - original draft. **Ismar de Souza Carvalho:** Writing – original draft, Resources.

## Declaration of competing interest

The authors declare that they have no known competing financial interests or personal relationships that could have appeared to influence the work reported in this paper.

## Data availability

Data shared in the supplementary material.

## Acknowledgments

The authors are grateful to I. T. Yamamoto, head of the paleontological division of the Agência Nacional the Mineração (ANM), for assistance in the authorization for collecting fossils in the Araripe Basin (ANM Process nº. 000.794/2015, Req. 007/2019). The fieldwork support was provided by José Artur Ferreira Gomes de Andrade (ANM) and Francisco Idalécio de Freitas (Araripe Geopark). Mauro Gabriel Passalia, an anonymous reviewer and the editor Francisco J. Vega are thankfully acknowledged for the help with greatly improving the manuscript.

## Appendix A. Supplementary data

Supplementary data to this article can be found online at https://doi.org/10.1016/j.jsames.2023.104331.

## References


Alvin, K.L., 1982. Cheirolepidiaceae: biology, structure and paleoecology. Rev. Palaeobot. Palynol. 37, 71–98.

Arai, M., Assine, M.L., 2020. Chronostratigraphic constraints and paleoenvironmental interpretation of the Romualdo Formation (Santana Group, Araripe Basin, northeastern Brazil) based on palynology. Cretac. Res. 116, 104610.

Assine, M.L., 2007. Bacia do Araripe. Bol. Geociencias Petrobras 15, 371–389.

Aucour, A.M., Gomez, B., Sheppard, S.M., Thévenard, F., 2008. $\delta^{13}C$ and stomatal number variability in the Cretaceous conifer *Frenelopsis*. Palaeogeogr. Palaeoclimatol. Palaeoecol. 257 (4), 462–473.

Barclay, R.S., Wing, S.L., 2016. Improving the *Ginkgo* $CO_2$ barometer: implications for the early Cenozoic atmosphere. Earth Planet Sci. Lett. 439, 158–171.

Barclay, R., McElwain, J., Dilcher, D., Sageman, B., 2007. The cuticle database: developing an interactive tool for taxonomic and paleoenvironmental study of the fossil cuticle record. Cour. Forschungsinst. Senckenberg 258, 39–55.

Barral, A., Gomez, B., Fourel, F., Daviero-Gomez, V., Lécuyer, C., 2017. $CO_2$ and temperature decoupling at the million-year scale during the Cretaceous Greenhouse. Sci. Rep. 7 (1), 1–7.

Batista, M.E.P., Martine, A.M., Saraiva, A.Á.F., Lima, F.J., Barros, O.A., Sá, A.A., Loiola, M.I.B., 2021. *Brachyphyllum*: state of the art and new data regarding *B. obesum*, the most representative fossil plant in the Araripe Basin, Brazil. J. S. Am. Earth Sci. 110, 103405.

Bernardes-de-Oliveira, M.E.C., Sucerquia, P.A., Mohr, B., Dino, R., Antonioli, L., Garcia, M.J., 2014. Indicadores paleoclimáticos na paleoflora do Crato, final do Aptiano do Gondwana Norocidental. In: Carvalho, I.S., Garcia, M.J., Lana, C.C., Strohschoen Jr, O. (Eds.), Paleontologia: Cenários de Vida e Paleoclimas, vol. 5. Interciência, Rio de Janeiro, pp. 101–119.

Berner, R.A., 2006. GEOCARBSULF: a combined model for Phanerozoic atmospheric $O_2$ and $CO_2$. Geochem. Cosmochim. Acta 70, 5653–5664.

Berner, R.A., 2008. Correction of "Inclusion of the weathering of volcanic rocks in the GEOCARBSULF model". Am. J. Sci. 308, 100–103.

Bétard, F., Peulvast, J.P., Magalhaes, A.O., Carvalho Neta, M.L., Freitas, F.I., 2018. Araripe Basin: a major geodiversity hotspot in Brazil. Geoheritage 10, 543–558.

Bottini, C., Erba, E., 2018. Mid-Cretaceous paleoenvironmental changes in the western Tethys. Clim. Past 14 (8), 1147–1163.

Carvalho, I.S., 2000. Geological environments of dinosaur footprints in the intracratonic basins of northeast Brazil during the Early Cretaceous opening of the South Atlantic. Cretac. Res. 21 (2–3), 255–267.

Carvalho, I.S., 2004. Dinosaur footprints from northeastern Brazil: taphonomy and environmental setting. Ichnos 11 (3–4), 311–321.

Carvalho, M.A., Lana, C.C., Sá, N.P., Santiago, G., Giannerini, M., Bengtson, P., 2022. Influence of the Intertropical Convergence Zone on Early Cretaceous plant distribution in the South Atlantic. Sci. Rep. 12 (1), 1–12.

César, S.N., Limarino, C.O., Llorens, M., Passalia, M.G., Pérez-Loinaze, V.S., Vera, E.I., 2011. High-precision late Aptian Pb/U age for the Punta del Barco Formation (Baqueró Group), Santa Cruz Province, Argentina. J. S. Am. Earth Sci. 31 (4), 426–431.

Chaboureau, A.C., Sepulchre, P., Donnadieu, Y., Franc, A., 2014. Tectonic-driven climate change and the diversification of angiosperms. Proc. Natl. Acad. Sci. USA 111 (39), 14066–14070.

Chaloner, W.G., McElwain, J.C., 1997. The fossil plant record and global climatic change. Rev. Palaeobot. Palynol. 95, 73–82.

Chumakov, N.M., Zharkov, M.A., Herman, A.B., Doludenko, M.P., Kalandadze, N.N., Lebedev, E.L., Ponomarenko, A.G., Rautian, A.S., 1995. Climatic belts of the mid-Cretaceous time. Stratigr. Geol. Correl. 3 (3), 42–63.

Dai, J., Sun, B., 2018. Early Cretaceous atmospheric $CO_2$ estimates based on stomatal index of *Pseudofrenelopsis papillosa* (Cheirolepidiaceae) from southeast China. Cretac. Res. 85, 232–242.

Davis, W.J., 2017. The relationship between atmospheric carbon dioxide concentration and global temperature for the last 425 million years. Climate 5 (4), 76.

Deng, S., Yang, X., Lu, Y., 2005. *Pseudofrenelopsis* (Cheirolepidiaceae) from the lower cretaceous of jiuquan, gansu, northwestern China. Acta Palaeontol. Sin. 44 (4), 505–516.

Dias, J.J., Carvalho, I.S., 2022. The role of microbial mats in the exquisite preservation of Aptian insect fossils from the Crato Lagerstätte, Brazil. Cretac. Res. 130, 105068.

Du, B., Sun, B., Zhang, M., Yang, G., Xing, L., Tang, F., Bai, Y., 2016. Atmospheric palaeo-$CO_2$ estimates based on the carbon isotope and stomatal data of Cheirolepidiaceae from the Lower Cretaceous of the Jiuquan Basin, Gansu Province. Cretac. Res. 62, 142–153.

El-Sharkawy, M.A., Cock, J.H., Del Pilar Hernandez, A., 1985. Stomatal response to air humidity and its relation to stomatal density in a wide range of warm climate species. Photosynth. Res. 7, 137–149.

Erba, E., Duncan, R.A., Bottini, C., Tiraboschi, D., Weissert, H., Jenkyns, H.C., Malinverno, A., 2015. Environmental Consequences of Ontong Java Plateau and Kerguelen Plateau Volcanism. The Origin, Evolution, and Environmental Impact of Oceanic Large Igneous Provinces, vol. 511. Geological Society of America Special Paper, pp. 271–303.

Fambrini, G.L., Silvestre, D.D.C., Barreto Junior, A.M., Silva-Filho, W.F.D., 2020. Estratigrafia da Bacia do Araripe: Estado da arte, revisão crítica e resultados novos. Geol. Usp. Série Científica 20 (4), 169–212.

Franks, P.J., Royer, D.L., Beerling, D.J., Van de Water, P.K., Cantrill, D.J., Barbour, M.M., Berry, J.A., 2014. New constraints on atmospheric $CO_2$ concentration for the Phanerozoic. Geophys. Res. Lett. 41 (13), 4685–4694.

Gan, Y., Zhou, L., Shen, Z.J., Shen, Z.X., Zhang, Y.Q., Wang, G.X., 2010. Stomatal clustering, a new marker for environmental perception and adaptation in terrestrial plants. Botanical Studies 51 (3), 325–336.

Gomes, J.M., Rios-Netto, A.M., Borghi, L., Carvalho, I.S., Mendonça Filho, J.G., Sabaraense, L.D., Araújo, B.C., 2021. Cyclostratigraphic analysis of the Early Cretaceous laminated limestones of the Araripe Basin, NE Brazil: estimating sedimentary depositional rates. J. S. Am. Earth Sci. 112, 103563.

Guerra-Sommer, M., Siegloch, A.M., Degani-Schmidt, I., Santos, A.C.S., Carvalho, I.S., Andrade, J.A.F.G., Freitas, F.I., 2021. Climate change during the deposition of the Aptian Santana Formation (Araripe Basin, Brazil): Preliminary data based on wood signatures. J. S. Am. Earth Sci. 111, 103462.

Haworth, M., Hesselbo, S.P., McElwain, J.C., Robinson, S.A., Brunt, J.W., 2005. Mid-Cretaceous $pCO_2$ based on stomata of the extinct conifer *Pseudofrenelopsis* (Cheirolepidiaceae). Geology 33 (9), 749–752.

Haworth, M., Heath, J., McElwain, J.C., 2010. Differences in the response sensitivity of stomatal index to atmospheric $CO_2$ among four genera of Cupressaceae conifers. Ann. Bot. 105 (3), 411–418.

Heimhofer, U., Hochuli, P.A., 2010. Early Cretaceous angiosperm pollen from a low-latitude succession (Araripe Basin, NE Brazil). Rev. Palaeobot. Palynol. 161 (3–4), 105–126.

Hofmann, C.C., Roberts, E.A., Seyfullah, L.J., 2022. Diversity of the dispersed gnetalean pollen record from the Lower Cretaceous Crato Formation, Brazil: entomophily, harmomegathy and habitat heterogeneity. Cretac. Res. 129, 105020.

Hoover, W.S., 1986. Stomata and stomatal clusters in *Begonia*: ecological response in two Mexican species. Biotropica 18, 16–21.

Jin, P., Zhang, M., Lei, X., Du, B., Dong, J., Sun, B., 2023. Testing multiple $pCO_2$ proxies from the Lower Cretaceous of the Laiyang Basin, eastern China. Cretac. Res. 141, 105352.

Jones, H.G., 2004. Application of thermal imaging and infrared sensing in plant physiology and ecophysiology. In: Callow, J.A. (Ed.), Advances in Botanical Research, vol. 41. Academic Press, pp. 107–163.

Kerp, H., 1990. The study of fossil gymnosperms by means of cuticular analysis. Palaios 5, 548–569.

Kidder, D.L., Worsley, T.R., 2010. Phanerozoic Large Igneous Provinces (LIPs), HEATT (Haline Euxinic Acidic Thermal Transgression) episodes, and mass extinctions. Palaeogeogr. Palaeoclimatol. Palaeoecol. 295 (1–2), 162–191.

Korn, R.W., 1993. Evidence in dicots for stomatal patterning by inhibition. Int. J. Plant Sci. 154 (3), 367–377.

Kunzmann, L., Mohr, B.A.R., Bernardes-de-Oliveira, M.E.C., Wilde, V., 2006. Gymnosperms from the Early Cretaceous Crato Formation (Brazil). II. Cheirolepidiaceae. Fossil Record 9 (2), 213–225.

Larkin, J.C., Marks, M.D., Nadeau, J., Sack, F., 1997. Epidermal cell fate and patterning in leaves. Plant Cell 9 (7), 1109–1120.

Llorens, M., Pérez-Loinaze, V., Passalia, M.G., Vera, E.I., 2020. Palynological, megafloral and mesofossil record from the Bajo Grande area (Anfiteatro de Ticó Formation, Baqueró Group, upper Aptian), Patagonia, Argentina. Rev. Palaeobot. Palynol. 273, 104137.

Martill, D.M., Bechly, G., Loveridge, R., 2007. The Crato Fossil Beds of Brazil: Window into an Ancient World. Cambridge University Press, Cambridge.

Matos, R.M.D., 1992. The northeast Brazilian rift. Tectonics 11, 766–791.

McElwain, J.C., 1998. Do fossil plants signal palaeoatmospheric $CO_2$ concentration in the geological past? Philosophical Transactions of the Royal Society B 353, 83–96.

McElwain, J.C., Chaloner, W.G., 1995. Stomatal density and index of fossil plants track atmospheric carbon dioxide in the Palaeozoic. Ann. Bot. 76, 389–395.

McElwain, J.C., Chaloner, W.G., 1996. The fossil cuticle as a skeletal record of environmental change. Palaios 11, 376–388.

Melo, R.M., Guzmán, J., Almeida-Lima, D., Piovesan, E.K., Neumann, V.H.D.M.L., 2020. New marine data and age accuracy of the Romualdo Formation, Araripe Basin, Brazil. Sci. Rep. 10 (1), 1–15.

Metcalfe, C.R., Chalk, L., 1979. Anatomy of the Dicotyledons, second ed. Clarendon Press, Oxford.

Mohr, B.A.R., Bernardes-de-Oliveira, M.E.C., Loveridge, R.F., 2007. The macrophyte flora of the Crato Formation. In: Martill, D.M., Bechly, G., Loveridge, R.F. (Eds.), The Crato Fossil Beds of Brazil: Window into an Ancient World. University Press, Cambridge, pp. 537–565.

Mohr, B.A.R., Schultka, S., Süss, H., Bernardes-de-Oliveira, M.E.C., 2012. A new drought resistant gymnosperm taxon *Duartenia araripensis* gen. nov. et sp. nov. (Cheirolepidiaceae?) from the Early Cretaceous of Northern Gondwana. Palaeontographica B 289 (1–3), 1–25.

Moisan, P., 2012. The study of cuticular and epidermal features in fossil plant impressions using silicone replicas for scanning electron microscopy. Palaeontol. Electron. 15 (2), 1–9.

Mora, G., Carmo, A.M., Elliott, W., 2021. Homeostatic response of Aptian gymnosperms to changes in atmospheric $CO_2$ concentrations. Geology 49 (6), 703–707.

Neumann, V.H., Cabrera, L., Mabesoone, J.M., Valença, L.M.M., Silva, A.L., 2002. Ambiente sedimentar e fácies da seqüência lacustre Aptiana–Albiana da bacia do Araripe, NE do Brasil. 6° Simpósio Sobre o Cretáceo Do Brasil. UNESP, Boletim, São Pedro 37–41.

Neumann, V.H., Borrego, A.G., Cabrera, L., Dino, R., 2003. Organic matter composition and distribution through the Aptian–Albian lacustrine sequences of the Araripe Basin, northeastern Brazil. Int. J. Coal Geol. 54 (1–2), 21–40.

Passalia, M.G., 2009. Cretaceous $pCO_2$ estimation from stomatal frequency analysis of gymnosperm leaves of Patagonia, Argentina. Palaeogeogr. Palaeoclimatol. Palaeoecol. 273 (1–2), 17–24.

Pellissier, L., Heine, C., Rosauer, D.F., Albouy, C., 2018. Are global hotspots of endemic richness shaped by plate tectonics? Biol. J. Linn. Soc. 123 (1), 247–261.

Pérez-Loinaze, V.S., Vera, E.I., Passalia, M.G., Llorens, M., Friedman, R., Limarino, C.O., Césari, S.N., 2013. High-precision U–Pb zircon age from the Anfiteatro de Ticó Formation: implications for the timing of the early angiosperm diversification in Patagonia. J. S. Am. Earth Sci. 48, 97–105.

Piovesan, E.K., Pereira, R., Melo, R.M., Guzmán, J., Almeida-Lima, D., Ramírez, J.D.V., Mouro, L.D., 2022. Organic inclusions in Brazilian Cretaceous amber: the oldest ostracods preserved in fossil resins. Cretac. Res. 131, 105091.

Poole, I., Kürchner, W.M., 1999. Stomatal density and index: the practice. In: Jones, T.P., Rowe, N.P. (Eds.), Fossil Plants and Spores: Modern Techniques. Geological Society, pp. 257–260.

Prado, G., Arthuzzi, J.C., Osés, G.L., Callefo, F., Maldanis, L., Sucerquia, P., Becker-Kerber, B., Romero, G.R., Quiroz-Valle, F.R., Galante, D., 2020. Synchrotron radiation in palaeontological investigations: examples from Brazilian fossils and its potential to South American palaeontology. J. S. Am. Earth Sci. 108, 102973.

Regali, M.S.P., Santos, P.S., 1999. Palinoestratigrafia e geocronologia dos sedimentos albo-aptianos das Bacias de Sergipe e Alagoas–Brasil. Simpósio sobre o Cretáceo do Brasil 5, 411–419.

Ribeiro, A.C., Ribeiro, G.C., Varejão, F.G., Battirola, L.D., Pessoa, E.M., Simões, M.G., Warren, L.V., Riccomini, C., Poyato-Ariza, F.J., 2021. Towards an actualistic view of the Crato Konservat-Lagerstätte paleoenvironment: a new hypothesis as an Early Cretaceous (Aptian) equatorial and semi-arid wetland. Earth Sci. Rev. 216, 103573.

Rios-Netto, A.M., Paula-Freitas, A.B.L., Carvalho, I.S., Regali, M.S.P., Borghi, L., Freitas, F.I., 2012. Formalização estratigráfica do Membro Fundão, Formação Rio da Batateira, Cretáceo Inferior da Bacia do Araripe, Nordeste do Brasil. Rev. Bras. Geociencias 42, 281–292.

Rothman, D.H., 2002. Atmospheric carbon dioxide levels for the last 500 million years. Proc. Natl. Acad. Sci. USA 99, 4167–4171.

Salisbury, E.J., 1927. I. On the causes and ecological significance of stomatal frequency, with special reference to the woodland flora. Phil. Trans. Roy. Soc. Lond. B 256 (431), 1–65.

Santos, A.C.S., Guerra-Sommer, M., Degani-Schmidt, I., Siegloch, A.M., Carvalho, I.S., Mendonca Filho, J.G., Mendonça, J.O., 2020. Fungus–plant interactions in Aptian Tropical Equatorial Hot arid belt: white rot in araucarian wood from the Crato fossil Lagerstätte (Araripe Basin, Brazil). Cretac. Res. 114, 104525.

Santos, A.C.S., Siegloch, A.M., Guerra-Sommer, M., Degani-Schmidt, I., Carvalho, I.S., 2021. *Agathoxylon santanensis* sp. nov. from the Aptian Crato fossil Lagerstätte, Santana Formation, Araripe Basin, Brazil. J. S. Am. Earth Sci. 112, 103633.

Scherer, C.M., Goldberg, K., Bardola, T., 2015. Facies architecture and sequence stratigraphy of an early post-rift fluvial succession, Aptian Barbalha Formation, Araripe Basin, northeastern Brazil. Sediment. Geol. 322, 43–62.

Scotese, C.R., Song, H., Mills, B.J., Van der Meer, D.G., 2021. Phanerozoic paleotemperatures: the Earth's changing climate during the last 540 million years. Earth Sci. Rev. 215, 103503.

Sewall, J.V., Van De Wal, R.S.W., Van Der Zwan, K., Van Oosterhout, C., Dijkstra, H.A., Scotese, C.R., 2007. Climate model boundary conditions for four Cretaceous time slices. Clim. Past 3 (4), 647–657.

Souza-Lima, W., Silva, R.O., 2018. Aptian–Albian paleophytogeography and paleoclimatology from Northeastern Brazil sedimentary basins. Rev. Palaeobot. Palynol. 258, 163–189.

Steinthorsdottir, M., Vajda, V., 2015. Early Jurassic (late Pliensbachian) $CO_2$ concentrations based on stomatal analysis of fossil conifer leaves from eastern Australia. Gondwana Res. 27 (3), 932–939.

Steinthorsdottir, M., Jardine, P.E., Rember, W.C., 2021. Near-future $pCO_2$ during the hot Miocene climatic optimum. Paleoceanogr. Paleoclimatol. 36, e2020PA003900.

Steinthorsdottir, M., Jardine, P.E., Lomax, B.H., Sallstedt, T., 2022. Key traits of living fossil *Ginkgo biloba* are highly variable but not influenced by climate – Implications for palaeo-$pCO_2$ reconstructions and climate sensitivity. Global Planet. Change 211, 103786.

Sucerquia, P.A., Bernardes-de-Oliveira, M.E.C., Mohr, B.A.R., 2015. Phytogeographic, stratigraphic, and paleoclimatic significance of *Pseudofrenelopsis capillata* sp. nov. from the Lower Cretaceous Crato Formation, Brazil. Rev. Palaeobot. Palynol. 222, 116–128.

Tajika, E., 1999. Carbon cycle and climate change during the Cretaceous inferred from a biogeochemical carbon cycle model. Isl. Arc 8 (2), 293–303.

Vakhrameev, V.A., 1981. Pollen *Classopollis*: indicator of Jurassic and Cretaceous climates. The Paleobotanist 28 (29), 301–307.

Vallejo, J.D., Piovesan, E.K., Carvalho, M.A., Guzmán, J., 2023. Palynofacies analyses of Santana Group, upper Aptian of the Araripe Basin, northeast Brazil: paleoenvironmental reconstruction. J. S. Am. Earth Sci. 121, 104154.

Van de Water, P.K., Leavitt, S.W., Betancourt, J.L., 1994. Trends in stomatal density and $^{13}C/^{12}C$ ratios of *Pinus flexilis* needles during last glacial-interglacial cycle. Science 264 (5156), 239–243.

Varejão, F.G., Silva, V.R., Assine, M.L., Warren, L.V., Matos, S.A., Rodrigues, M.G., Fürsich, F.T., Simões, M.G., 2020. Marine or freshwater? Accessing the paleoenvironmental parameters of the Caldas Bed, a key marker bed in the Crato Formation (Araripe Basin, NE Brazil). Braz. J. Genet. 51, 1–12.

Woodward, F.I., 1987. Stomatal numbers are sensitive to increases in $CO_2$ from pre-industrial levels. Nature 327 (6123), 617–618.

Yang, X., Deng, S., 2007. Discovery of *Pseudofrenelopsis gansuensis* from the Lower Cretaceous of Wangqing, Jilin Province, and its significance in correlation of Cretaceous red beds in China. Acta Geologica Sinica-English Edition 81 (6), 905–910.

Ziegler, A., Eshel, G., Rees, P.M., Rothfus, T., Rowley, D., Sunderlin, D., 2003. Tracing the tropics across land and sea: Permian to present. Lethaia 36 (3), 227–254.